Declaration of Academic Integrity

to be used throughout the University from 2012-13
for submitted work at undergraduate and taught postgraduate levels:

I promise that in the attached submission I have not presented or attempted to present anyone else's work as my own except where I have explicitly so indicated. I understand that to do so would mean that I had committed plagiarism, the University's definition of which is published. I know that if I commit plagiarism I can be expelled from the University and that it is my responsibility to be aware of the University's regulations on plagiarism and their importance.

I re-confirm my consent to the University copying and distributing any or all of my work in any form and using third parties (who may be based outside the EU/EEA) to monitor breaches of regulations, to verify whether my work contains plagiarised material, and for quality assurance purposes.

I confirm that I have declared all mitigating circumstances that may be relevant to the assessment of this piece of work and that I wish to have taken into account. I am aware of the School's policy on mitigation and procedures for the submission of statements and evidence of mitigation. I am aware of the penalties imposed for the late submission of coursework.

Full Name: IAN ALEXANDER EDWARD CULLEN   Student Number: 200485506

Signed: IaCu   Date: 22/04/13

Plagiarism is defined as presenting someone else's work as your own. Work means any intellectual output, and typically includes text, data, images, sound or performance, or any combination of these.

A Prediction of the Geo-neutrino Flux at SNOLAB

Ian A. E. Cullen
School of Physics and Astronomy, University of Leeds.
Leeds, United Kingdom, LS2 9JT

Abstract

It is believed that a large fraction of the heat produced by the Earth could originate due to the decay of radioactive elements. A signature of this decay should be visible to us at the surface in the form of the flux of antineutrinos. Therefore the geo-neutrino flux is of fundamental importance in the field of geophysics where it is believed that it will enable us to determine the amount and possibly location of heat producing elements within the Earth. SNO+ will begin gathering data later this year, including a measurement of the geo-neutrino flux. In this study we outline the method employed to predict the geo-neutrino flux that will be present at SNO+ and use this to estimate the signal rate that will observed. We predict that the total geo-neutrino flux at SNO+ will be $(5.27 \pm 0.31) \times 10^{10}\mathrm{m}^{-2}\mathrm{s}^{-1}$ corresponding to a signal rate of (45.6 ± 2.7) TNU. In addition the MSW effect was considered and was found to reduce the geo-neutrino signal rate to (41.5 ± 11) TNU. Good agreement was observed not only between these results and those predicted in previous studies, but also the flux predicted for the locations of previous geo-neutrino experiments, Kamioka and Gran Sasso, demonstrated concurrence with the experimental results.

Contents

1. Introduction

The existence of the particle we now know as a neutrino was first suggested in 1930 by Wolfgang Pauli [1] who proposed that a third particle, in addition to the proton and beta particle, must be produced in beta decays in order to explain the spectrum of beta energies observed. We now know that this prediction was correct, but that the particle he proposed was in fact the electron antineutrino. However at the time neutrinos were incredibly difficult to observe due to their small interaction cross section, indeed after estimating a neutrino cross-section of $\sigma < 10^{-44}\text{cm}^2$ in 1934 Bethe concluded there was no practical way to detect the neutrino [2]. This was proved to be untrue in 1956 when Cowan *et al* succeeded in detecting neutrinos produced in a nuclear reactor by searching for coincidence between the interactions of the two inverse beta decay products [3]. It is now known that the reason neutrinos proved difficult to detect is due to their low mass and lack of charge, causing them to interact primarily through the weak force.

Geo-neutrinos are electron antineutrinos that are produced during the beta decay of radioactive elements within the Earth. The idea that the earth should be producing large quantities of geo-neutrinos was first suggested by Eder in 1966 [4]. It is believed that the radioactive elements within the Earth should produce antineutrinos when they decay which ought to in theory be measurable to us at the surface thanks to the highly penetrating nature of neutrinos. Presently the study of geo-neutrinos is a considerably active area of research in the physics community. It brings together the fields of high energy physics and geophysics in order to help answer some fundamental issues such as the source of the Earth's internal heat.

It is well known that the Earth is emitting heat, in [5] it is estimated that the total heat flow from the Earth is 44.2 ± 1TW. While it is difficult to fully quantify the sources of this heat it is unlikely that it can be completely explained by the energy released from the gravitational collapse during the formation of the Earth. This energy is estimated to be 2.24×10^{32} J using the gravitational binding energy for a sphere as seen in equation 1, which if lost a constant rate could account for the heat flow seen today. However as the Earth formed slowly from an accretion disc it is likely that a large fraction of this energy would have been lost during this formation period and hence the fraction due to gravitational energy now is likely to be much smaller.

$$U_{grav} = \frac{3GM_{\oplus}^2}{5R_{\oplus}} \tag{1}$$

Presently it is believed that radioactive decays could contribute a large portion of the Earth's heat; an estimate of the fraction of the heat produced by radioactive decays is 21 ± 4TW, obtained by assuming similarities between the content of the Earth and chondritic meteorites [6]. However one cannot directly measure the amount of radioactive nuclides in the Earth, the deepest hole that has ever been dug is a mere 12km [7], and therefore we rely on indirect methods. As geo-neutrinos are produced in radioactive decays, and due to their aforementioned small cross-section, it is believed they can carry information about the distribution of the heat producing elements to the surface. By carrying out experiments to measure the geo-neutrino flux one can estimate the abundances of the radioactive elements within the earth, which can be used as an analysis of the various Earth models.

So far there have been two experimental studies on geo-neutrinos; SNO+ will be the third when it begins taking data later this year [8]. The primary method of detecting geo-neutrinos is via inverse beta decay, illustrated by equation 2, whereby an electron antineutrino converts a proton into a neutron and creates a positron.

$$\nu_e + p \rightarrow n + e^+ \tag{2}$$

As with the experiment by Cowan *et al*, the modern day approach to detecting geo-neutrinos in a liquid scintillator is to look for coincidence between the two photons emitted. The first by the annihilation of the emitted positron with an electron, and the second by the capture of the neutron by a proton, which on average occurs approximately $200\mu s$ later. However due to the mass difference between the proton and the products, this interaction imposes a neutrino energy threshold of 1.806MeV. There are thought to be three main isotopes of heat producing elements (HPE) within the Earth, ^{238}U, ^{232}Th and ^{40}K. The maximal neutrino energy in either of the ^{40}K decay chains is 1.311MeV, preventing geo-neutrinos produced by Potassium from being detectable via this method.

The first reported experimental detection of geo-neutrinos was by the KamLAND collaboration in 2005 based on results obtained from the Kamioka Observatory in Japan. In [9] they claim a detected total geo-neutrino flux of $1.62 \times 10^7 \text{cm}^{-2} s^{-1}$ at the 99% confidence level. KamLAND is a 1kton liquid scintillator based detector located 1km underground. Like most current geo-neutrino experiments the main form of detection is to look for scintillation light produced by the positron emitted in an inverse beta decay event. However it must be noted that due to the large difficulty in separating geo-neutrino events from others such as reactor and background neutrinos, the validity of these results merits questioning. The number of geo-neutrino events detected over the runtime of 749.1 ± 0.5 days is reported to be between 4.5 and 54.2 at the 90% confidence level. Therefore based on these results alone it is debatable as to whether this experiment truly does show geo-neutrino detections at all.

The second experiment to report geo-neutrino detections is that by the Borexino collaboration [10]. The detector at Borexino is located at the Gran Sasso National Laboratory in Italy. The detector itself is similar to that used at KamLAND, consisting of a vessel filled with liquid scintillator and surrounded by photo-multiplier tubes, although the containment vessel at Borexino is less than a third of the diameter of that at KamLAND. Also as with KamLAND, the method for detection of geo-neutrino is the inverse beta decay. At Borexino they report detecting $9.9^{+14.6}_{-8.2}$ geo-neutrino events at the 3σ confidence level over the course of their measurements. Although once again this is a fairly large uncertainty, it does likely suggest the actual detection of a geo-neutrino. While Borexino does not suffer quite so much as KamLAND from the presence of reactor neutrinos, it is limited by its relatively small detector which will reduce the chance of detecting a geo-neutrino.

The difficulty in accurately determining whether an event was caused by a geo-neutrino is due to fake events being caused by alternative sources of neutrinos in the same energy range. There are two main causes of these fake events. The first is background neutrinos whereby contaminants have entered the detector, most likely from the liquid scintillator, which then decay after a time emitting a neutrino. And secondly reactor neutrinos which are neutrinos emitted from nearby fission reactors. The latter is a particularly large source of uncertainty for the KamLAND experiment where at the time of measurement there were 21 reactors within 200km alone [7]. One of the key sources of background neutrinos arises from ^{222}Rn contamination in the detector. Through this decay chain alpha particles will be emitted which produce neutrons through the $^{13}\text{C}(\alpha, n)^{16}\text{O}$ reaction. It is estimated that a large source of uncertainty in the KamLAND experiment comes from predicting the cross section, and hence likelihood of occurrence, for this reaction. The cross section employed by KamLAND was that given by JENDL [11] which gives an uncertainty in the cross section of 20%. However if one uses the value given by [12] the uncertainty in this measurement drops to 4%, which leads to a count of 31^{+14}_{-13} geo-neutrino events at KamLAND. This result suggests the detection of geo-neutrinos with much higher confidence.

As a measurement of the geo-neutrino flux can be used to analyse the structure of the Earth, the reverse is also true; the geo-neutrino flux at a given location can be predicted based on accurate models of the Earth. The aim of this study was to predict the geo-neutrino flux at SNOLAB in Sudbury, Canada. While the main aims of SNO+ are in other areas of neutrino physics such as the hunt for the illusive neutrinoless double beta decay it will also function well as a geo-neutrino detector. The SNO+ detector will be a similar set-up to that employed in both KamLAND and Borexino but with a 12m diameter vessel containing 780tons of liquid scintillator. In addition to being a considerably larger detector than Borexino, it is estimated that the flux from reactor neutrinos will be a factor 5 times less than that present at KamLAND [8]. Additionally it is believed the relatively thick continental crust near SNO+ compared to KamLAND should yield a larger geo-neutrino flux which in turn will be more easily distinguishable from the various backgrounds.

In the following section we shall detail the methods used in order to calculate the geo-neutrino flux and signal at SNO+ and other locations. This consists of an analysis of the Earth models used, a method for calculating the survival probability of geo-neutrinos, the energy spectrum for geo-neutrinos and an approach for estimating the geo-neutrino signal rate from the flux. We shall then present the results obtained for the geo-neutrino flux and signal rate at SNO+ and other locations. Finally we will thoroughly discuss our results including the relative effects caused by the assumptions that were employed.

2. Method

The flux of geo-neutrinos of energy $E_{\bar{\nu}}$, originating from an element X and arriving at a location $\vec{R}$ is given by the following integration over the volume of the Earth

$$\phi_X^{arr}(E_{\bar{\nu}}) = \int_{V_\oplus} dV \frac{\rho(\vec{r})}{4\pi|\vec{R}-\vec{r}|^2} \frac{a_X(\vec{r})C_X}{\tau_X m_X} f_X(E_{\bar{\nu}}) P_{ee}(E_{\bar{\nu}}, |\vec{R}-\vec{r}|) \tag{3}$$

Here $\rho(\vec{r})$ represents the density of the Earth at a given point, $a_X(\vec{r})$ is the abundance of element X at this point, and C_X, τ_X, and m_X are the concentration, lifetime and mass of the neutrino producing isotope of this element. The factor $f_X(E_{\bar{\nu}})$ represents the normalised neutrino energy spectrum produced by the decay chain of element X and $P_{ee}(E_{\bar{\nu}}, |\vec{R}-\vec{r}|)$ is the survival probability of an electron antineutrino of given energy that has travelled a certain distance. As mentioned previously, there are just two relevant isotopes of HPEs that will emit detectable geo-neutrinos, Uranium and Thorium. This allowed the following simplification to be made in that we reduced the factor that governs the neutrino rate to just one value for each element as per equation 4.

$$\epsilon_X = \frac{C_X}{\tau_X m_X} \tag{4}$$

Where the values used for the relevant isotopes in this study were $\epsilon_{\mathrm{U}} = 7.41 \times 10^7 \mathrm{kg}^{-1}\mathrm{s}^{-1}$ and $\epsilon_{\mathrm{Th}} = 1.62 \times 10^7 \mathrm{kg}^{-1}\mathrm{s}^{-1}$ [7].

2.1. Earth Model

The flux of geo-neutrinos at the surface depends heavily on the structure and composition of the Earth, in the form of the density and abundance of HPEs. However as mentioned previously one cannot directly measure either of these parameters to any meaningful depth. Therefore in order to predict the geo-neutrino flux we rely on indirect methods to produce a density profile for the Earth. In this study we chose to use the Preliminary Reference Earth Model (PREM) [13] for the density of the inner layers of the Earth. The PREM is the result of a committee set up to create a standard Earth model for future use in the scientific community. It consists of an isotropic model of the Earth divided into nine layers, wherein the density is calculated by analysis of seismology. The densities from the PREM used in this study can be seen in table 1, obtained by fitting a polynomial to the radius dependant density estimations. While the assumption of isotropy presents a convenient solution to work with, it is suggested in the paper that it does not strictly fit all data, indeed it is observed that for the crust itself averaging over the anisotropies creates a result that is unlike any part of the real crust. In the case of calculating geoneutrino flux, the inverse square of the distance weighting necessitates that the local region of the detector be known accurately therefore this model, while suitable for the inner areas of the Earth, needs refinement before it can be applied to the crust. For this reason the outer layers of the Earth were described in this study using the CRUST2.0 model [14]. This model features a more advanced description of the crust, releasing the assumption of isotropy by defining the properties of the crust on a 2x2 degree scale. The CRUST2.0 model defines the crust in terms of seven layers, combining these with the PREM components yields the complete Earth model assumed in this study, as shown in figure 1.

Region	Radius (km)	Density ($\mathrm{g\,cm^{-3}}$)
Inner core	$0 - 1221.5$	$13.0885 - 8.8381x^2$
Outer core	$1221.5 - 3480.0$	$12.5815 - 1.2638x - 3.6426x^2 - 5.5281x^3$
Lower mantle	$3480.0 - 5701.0$	$7.9565 - 6.4761x + 5.5283x^2 - 3.0807x^3$
Upper mantle	$5701.0 - 5771.0$	$5.3197 - 1.4836x$
	$5771.0 - 5971.0$	$11.2494 - 8.0298x$
	$5971.0 - 6151.0$	$7.1089 - 3.8045x$
	$6151.0 - 6346.6$	$2.6910 + 0.6924x$
Lower crust	$6346.6 - 6356.0$	2.900
Upper crust	$6356.0 - 6368.0$	2.600

Table 1: The density values taken from the PREM where $x = r/\bar{R}$ and the Earth mean radius is taken to be $\bar{R} = 6371.0$km

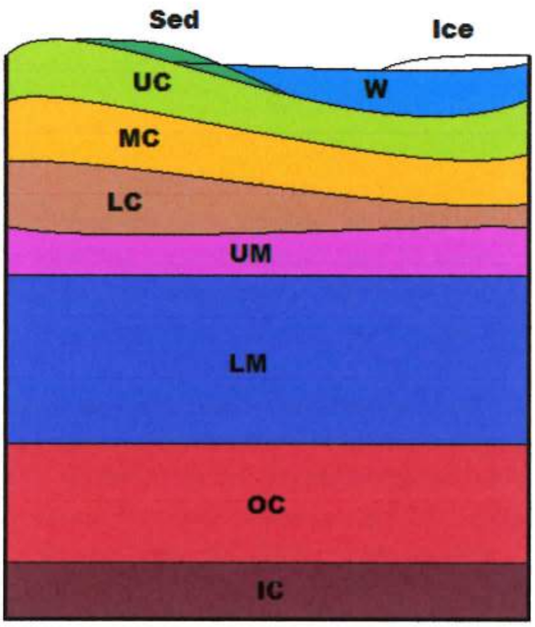

Figure 1: Schematic of the Earth Model used in this study. The inner core (IC), outer core (OC), lower mantle (LM) and upper mantle (UM) are defined isotropically as in the PREM. The remaining layers, the lower crust (LC), the middle crust (MC), the upper crust (UC), the sediments (Sed), water (W) and ice are defined in three dimensions as in the CRUST2.0 model. The discontinuity between the upper mantle and lower crust, known as the Moho, is also the three dimensional boundary between the two models.

As with density the position dependant abundance of HPEs in the Earth is impossible to measure directly. We therefore rely on indirect methods to estimate the average abundance in each of the Earth layers. The abundances in the sediments are obtained from a paper by Plank and Langmuir [15]. These are calculated by averaging over local values obtained through either direct measurement of sediment composition or by using known correlations between the HPEs and other elements such as Aluminium. The composition used for the continental crust in this study was taken from [16]. The upper crustal abundances are found by studying trends between these elements and Lathanum in Loess, a type of sediment, while the abundances in the middle crust are calculated by averaging over previous studies. The lower continental crust abundances are taken directly from a previous study [17]. The abundances for the oceanic crust and mantle elements are given in [18]. These values are found by reviewing studies on the topic and choosing either the most accurate or an average of the results. For the core it is estimated that there is no uranium or thorium present [6] based on the fact that these elements are by nature lithophilic and hence will not be found in the core. A summary of the abundances used can be seen in table 2.

Earth Section		Abundances		Source
		Uranium	Thorium	
Sediments	Continental	2.8	10.7	[15]
	Oceanic	1.68	6.91	
Continental Crust	Upper	2.7 ± 0.6	10.5 ± 1.0	[16]
	Middle	1.3 ± 0.4	6.5 ± 0.5	
	Lower	0.2	1.2	[17]
Oceanic Crust		0.10 ± 0.03	0.22 ± 0.07	[18]
Mantle (ppb)	Upper	3.95 ± 1.2	10.8 ± 3.2	[18]
	Lower	17.3 ± 4.7	60.4 ± 16.3	
Core		0	0	[6]

Table 2: The abundances of Uranium and Thorium found inside the Earth, values are in ppm by mass ($\mu g/g$) unless stated otherwise

2.2. Neutrino Oscillations

In order to calculate the geo-neutrino flux as given by equation 3, the survival probability for a neutrino of given energy after travelling a given distance must be known. Despite the small interaction cross-section of neutrinos, this probability is not unitary due to the phenomenon of neutrino oscillations. A long standing issue in particle physics was the so called Solar Neutrino Problem, whereby a deficit in the predicted number of solar neutrinos was observed. It is now believed that this phenomenon can be explained if one allows the neutrinos to oscillate between flavour states. This effect was first quantified by Maki *et al* in 1962 [19] where mixing between two flavour states was proposed. We now know that neutrino mixing is a consequence of each of the three neutrino flavour states consisting of a superposition of the three mass states. As a neutrino propagates the mass eigenstates evolve independently which causes the proportion of each mass state and hence the flavour states to alter. The relationship between the flavour states and mass states is given by the mixing matrix U, the form of which used in this study is seen in equation 5, taken from [20].

$$\begin{pmatrix} \bar{\nu}_e \\ \bar{\nu}_\mu \\ \bar{\nu}_\tau \end{pmatrix} = \begin{pmatrix} c_{12}c_{13} & s_{12}c_{13} & s_{13} \\ -s_{12}c_{23} - c_{12}s_{23}s_{13} & c_{12}c_{23} - s_{12}s_{23}s_{13} & s_{23}c_{13} \\ s_{12}s_{23} - c_{12}s_{23}s_{13} & -c_{12}s_{23} - s_{12}c_{23}s_{13} & c_{23}c_{13} \end{pmatrix} \begin{pmatrix} \bar{\nu}_1 \\ \bar{\nu}_2 \\ \bar{\nu}_3 \end{pmatrix} \tag{5}$$

The convention used is that $s_{ij} = \sin(\theta_{ij})$ and $c_{ij} = \cos(\theta_{ij})$, where θ_{ij} represents the mixing angle between two mass states i, j. This form of the mixing matrix ignores the CP violating phase factor δ based on the fact that it has not been experimentally confirmed as of yet. This allows the survival probability of an electron antineutrino with energy $E_{\bar{\nu}}$ after travelling a distance L to be calculated from equation 6.

$$P_{ee} = 1 - 4 \sum_{i>j=1}^{3} U_{ei}^2 U_{ej}^2 \sin^2\left(\frac{\Delta m_{ij}^2 L}{4E_{\bar{\nu}}}\right) \tag{6}$$

However as one of the three mass differences remains unknown it was chosen to use the hierarchical model whereby it was assumed that $\Delta m_{23}^2 \approx \Delta m_{13}^2 \gg \Delta m_{12}^2$. This allows the survival probability for electron antineutrinos in a vacuum to be approximated as equation 7.

$$P_{ee} = 1 - \sin^2(2\theta_{12})\cos^4(\theta_{13})\sin^2\left(\frac{\Delta m_{12}^2 L}{4E_{\bar{\nu}}}\right) - \sin^2(2\theta_{13})\sin^2\left(\frac{\Delta m_{13}^2 L}{4E_{\bar{\nu}}}\right) \tag{7}$$

The mixing parameters used in this study were obtained from a review by the Particle Data Group [21]. They were $\Delta m_{12}^2 = (7.50 \pm 0.20) \times 10^{-5}\text{eV}^2$, $\Delta m_{13}^2 = \left(2.32^{+0.12}_{-0.08}\right) \times 10^{-3}\text{eV}^2$, $\sin^2(2\theta_{12}) = 0.857 \pm 0.024$, $\sin^2(2\theta_{13}) = 0.098 \pm 0.013$ and $\sin^2(2\theta_{23}) = 0.95$.

The survival probability given in equation 7 assumes that the neutrinos do not interact with their surroundings as they pass through the Earth. However the possibility that the oscillations between flavour states of neutrinos, and hence survival probability, might be affected by interactions with surrounding matter was proposed by Wolfenstein in 1978 [22]. This matter effect on neutrino oscillations is now known as the MSW effect after it's three original proponents, Mikheyev, Smirnov and Wolfenstein. For the case of solar neutrinos the MSW effect has now been experimentally confirmed by SNO [23]. On the other hand due to the lower density of matter in the Earth, relative to the Sun, the effect has yet to be observed for neutrinos passing through the Earth. Despite this we propose a method to predict the consequence of the MSW effect on geo-neutrinos. As a geo-neutrino propagates through the Earth it will interact via the weak force with electrons in the matter. There are two forms of this weak interaction, the neutral current interaction which occurs through the exchange of a Z boson and the charged current interaction which is mediated by the W boson. These are shown diagrammatically in figure 2.

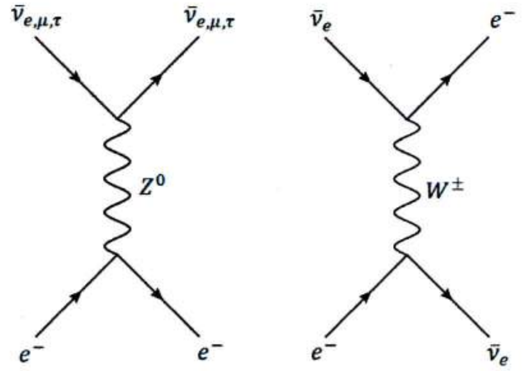

Figure 2: The neutral current (a) and charged current (b) interactions of antineutrinos with Earth matter. While all three flavours can undergo the neutral current interaction, only the electron antineutrino can undergo the charged current interaction. Time runs horizontally.

As only the electron antineutrino can undergo the charged current interaction, due to lepton number conservation, this introduces a potential only felt by the electron flavour state. This potential causes an alteration to the electron antineutrino propagation with respect to in a vacuum, and as such will cause the survival probability of geo-neutrinos to change. In order to describe this effect mathematically it is necessary to first introduce the Hamiltonian for neutrinos in a vacuum and as measured in the mass basis.

$$H^i = \frac{1}{2E_{\bar{\nu}}} \begin{pmatrix} 0 & 0 & 0 \\ 0 & \Delta m^2_{21} & 0 \\ 0 & 0 & \Delta m^2_{31} \end{pmatrix} \tag{8}$$

This can then be transformed into the flavour basis via the relationship $H^\alpha = U^\dagger H^i U$, where U is the mixing matrix as defined in equation 5. The potential for the matter interaction can then be included to obtain the complete time dependant Hamiltonian for neutrinos passing through matter as measured in the flavour basis.

$$H^\alpha_m(t) = U^\dagger H^i U + \frac{1}{2E_{\bar{\nu}}} \begin{pmatrix} a(t) & 0 & 0 \\ 0 & 0 & 0 \\ 0 & 0 & 0 \end{pmatrix} \tag{9}$$

Where $a(t)$ represents the charged current potential felt only by the electron antineutrino. The form of this potential at a location within the Earth x is given in [24] and has the form shown in equation 10.

$$a(x) = 2\sqrt{2}G_F E_{\bar{\nu}} n_e(x) \approx 7.56 \times 10^5 \mathrm{eV}^2 \left(\frac{\rho(x)}{\mathrm{gcm}^{-3}}\right)\left(\frac{E_{\bar{\nu}}}{\mathrm{GeV}}\right) \tag{10}$$

Where G_F and $n_e(x)$ denote the Fermi constant and electron number density respectively. The neutrino equation of state is then given by the following Schrödinger equation.

$$i\hbar\frac{d}{dt}|\bar{\nu}_\alpha(t) >= H^\alpha_m(t)|\bar{\nu}_\alpha(t) > \quad \text{where} \quad |\bar{\nu}_\alpha(t) >= \begin{pmatrix} \bar{\nu}_e(t) \\ \bar{\nu}_\mu(t) \\ \bar{\nu}_\tau(t) \end{pmatrix} \tag{11}$$

Here the neutrino state vector contains elements which are effectively the probabilities of finding the neutrino in a given flavour state after a time t. The general solution to this Schrödinger equation is as follows.

$$|\bar{\nu}_\alpha(t) >= e^{-\frac{i}{\hbar}\int_0^t H^\alpha_m(t')dt'} |\bar{\nu}_\alpha(0) > \tag{12}$$

The integral in equation 12 can then be trivially converted to that over the path of the neutrino by assuming that the neutrinos travel at the speed of light. This allows the integration to be calculated using the following.

$$\int_0^t H^\alpha_m(t')dt' = \frac{L}{c}U^\dagger H^i U + \frac{1}{2E_{\bar{\nu}}c} \begin{pmatrix} \int_0^L a(x)dx & 0 & 0 \\ 0 & 0 & 0 \\ 0 & 0 & 0 \end{pmatrix} \tag{13}$$

If the operator in equation 13 commutes with itself at two different times or equivalently at two different locations then this produces the neat solution seen in equation 14.

$$|\bar{\nu}_\alpha(E_{\bar{\nu}}, x) >= \sum_i e^{\lambda_i(E_{\bar{\nu}}, x)}|\lambda_i(E_{\bar{\nu}}, x) >< \lambda_i(E_{\bar{\nu}}, x)|\bar{\nu}_\alpha(0) > \tag{14}$$

Where $\lambda_i(E_{\bar{\nu}}, x)$ and $|\lambda_i(E_{\bar{\nu}}, x) >$ are the eigenvalues and eigenvectors of the operator in equation 13 for a antineutrino of energy $E_{\bar{\nu}}$ evaluated at a position x. However it was found that this operator only commuted at two different positions x and x' if $a(x) = a(x')$, specifically that the density needed to be homogeneous along the neutrino path. In order to save on computation time the assumption was made that the density observed for each geo-neutrino was constant along its path, and equal to the average density along this path. This allowed the use of equation 14 and hence allowed the final geo-neutrino state to be calculated by using the fact that the initial state was known to be that of an electron-antineutrino. The survival probability could then be calculated for an antineutrino passing through matter using equation 15.

$$P_{ee}(E_{\bar{\nu}}, L) = |<\bar{\nu}_e|\bar{\nu}_\alpha(E_{\bar{\nu}}, L)>|^2 \quad \text{where} \quad |\bar{\nu}_e>=|\bar{\nu}_\alpha(0)>= \begin{pmatrix} 1 \\ 0 \\ 0 \end{pmatrix} \tag{15}$$

2.3. Geo-neutrino Spectrum

The geo-neutrino flux in equation 3 is dependant on the neutrino energy in the form of the survival probability. This made it necessary to constrain the antineutrino spectrum seen due to beta decay so that the relative probability of a geo-neutrino with given energy being emitted could be calculated. The antineutrino spectrum used in this study was obtained using the method outlined in [7]. The antineutrino spectrum $f_{i,k;k}(E_{\bar{\nu}})$ for a beta decay from nuclide i to j into a state k can be obtained from the corresponding well-known electron spectrum $\phi_{i,j;k}(W)$ using energy conservation such that

$$f_{i,j;k}(E_{\bar{\nu}}) = \phi_{i,j;k}(W) \quad \text{where} \quad W = W_{max} - E_{\bar{\nu}} \tag{16}$$

The electron energy W has an upper limit of $W_{max} = m_e c^2 + E_{max}$ where E_{max} is the maximum energy available to the antineutrino for the given transition $i \rightarrow j$. The antineutrino spectrum in equation 16 could then be calculated using the following form for the electron spectrum

$$\phi_{i,j;k}(W) = \frac{1}{N} W(W_{max} - W)^2 (W^2 - m_e^2 c^4)^{\gamma - 1/2} e^{\pi y} \left|\Gamma(\gamma + iy)\right|^2 \tag{17}$$

$$\gamma = \sqrt{1 - (\alpha Z)^2}, \quad y = \alpha Z \frac{W}{\sqrt{W^2 - m_e^2 c^4}} \tag{18}$$

Using the knowledge that α is the fine structure constant, Z is the charge of the daughter nucleus and N is a normalisation constant, this allowed the geo-neutrino spectrum to be calculated which in turn allowed the calculation of the energy dependant geo-neutrino flux.

2.4. Flux Calculation

With all the components of equation 3 obtained the arrival flux could be calculated. For this we used the Monte Carlo VEGAS algorithm from the GNU Software Library. This is an adaptive numerical integration routine and as such attempts to focus the integration arguments into the areas of highest variation in order to improve the accuracy of the result. The integration was performed separately over a number of cones of differing angular direction with respect to the detector, and the results for each summed to obtain the total flux. This allowed the relationship between flux and angle of incidence to be probed, as in principal it may be possible to determine the direction of propagation of detected geo-neutrinos. This would allow further tests of Earth models as it would allow the differentiation between the geo-neutrinos produced from the crust, which would primarily enter the detector laterally, and the mantle produced geo-neutrinos which would come from lower angles.

2.5. Geo-neutrino Signal

The number of expected geo-neutrino events at SNO+ can be estimated based on the neutrino flux, the relevant cross-section and the properties of the SNO+ detector. In [7] the geo-neutrino signal produced from an element X is given as

$$S(X) = N_p \int dE_{\bar{\nu}} \varepsilon(E_{\bar{\nu}}) \sigma(E_{\bar{\nu}}) \phi_X^{arr}(E_{\bar{\nu}}) \tag{19}$$

where N_p is the number of target protons inside the detector, $\varepsilon(E_{\bar{\nu}})$ is the efficiency of the antineutrino detection process, which in principal depends on the neutrino energy, $\sigma(E_{\bar{\nu}})$ is the antineutrino - proton cross-section and $\phi_X^{arr}(E_{\bar{\nu}})$ is the geo-neutrino flux arriving at the detector as given by equation 3.

As mentioned previously the primary method of detecting geo-neutrinos is via the inverse beta decay process (2). The cross-section for this antineutrino - proton interaction, neglecting the neutron recoil is given in [25] as

$$\sigma(E_{\bar{\nu}}) = \frac{2\pi^2\hbar^3}{m_e^5 c^8 f \tau_n}(E_{\bar{\nu}} - \Delta M c^2)\left[(E_{\bar{\nu}} - \Delta M c^2)^2 - (m_e c^2)^2\right]^{1/2} \tag{20}$$

where f and τ_n are the phase space factor and lifetime of the neutron beta decay and are found to be 1.71465 ± 0.00015 [26] and (880.1 ± 1.1)s [21]. $\Delta M = (1.29333217 \pm 0.00000042)$MeV is the neutron-proton mass difference [21]. Based on the assumption that SNO+ will be a similar detector to that employed at KamLAND, the approximation was made that the efficiency of the two detectors would be roughly equal, and independent of energy within the geo-neutrino energy range. This allowed the efficiency of SNO+ to be approximated as $\varepsilon = 0.687 \pm 0.007$ as was used by KamLAND [9]. However, this calculation could be further simplified by instead using an average cross-section as in [7]. We defined an average cross-section for each of the two HPEs, such that $<\sigma>_{\mathrm{U}} = 0.404 \times 10^{-44}\mathrm{cm}^2$ and $<\sigma>_{\mathrm{Th}} = 0.127 \times 10^{-44}\mathrm{cm}^2$. This allowed a signal rate to be calculated per 10^{32} target protons using the following equations.

$$\frac{S(^{238}\mathrm{U})}{10^{32}\mathrm{protons}} = 4.04 \times 10^{-7}\mathrm{s}^{-1} \times \varepsilon \left(\frac{\Phi_{\mathrm{U}}^{arr}}{10^6\mathrm{cm}^{-2}\mathrm{s}^{-1}}\right) \tag{21}$$

$$\frac{S(^{232}\mathrm{Th})}{10^{32}\mathrm{protons}} = 1.27 \times 10^{-7}\mathrm{s}^{-1} \times \varepsilon \left(\frac{\Phi_{\mathrm{Th}}^{arr}}{10^6\mathrm{cm}^{-2}\mathrm{s}^{-1}}\right) \tag{22}$$

Where Φ_X^{arr} represents the total energy integrated geo-neutrino flux arriving at the detector due to a HPE X.

3. Results

We predict a geo-neutrino flux due to Uranium of $(2.80 \pm 0.12) \times 10^{10}\mathrm{m}^{-2}\mathrm{s}^{-1}$ when using the vacuum survival probability as given in equation 7. This falls to $(2.55 \pm 0.50) \times 10^{10}\mathrm{m}^{-2}\mathrm{s}^{-1}$ when considering the MSW effect as in equation 15. These results correspond to a predicted signal rate of 24.5 TNU and 22.3 TNU respectively where the terrestrial neutrino unit (TNU) is defined as one event per 10^{32} target protons per year. For Thorium the predicted flux is $(2.47 \pm 0.10) \times 10^{10}\mathrm{m}^{-2}\mathrm{s}^{-1}$ when using the vacuum survival probability and $(2.25 \pm 0.43) \times 10^{10}\mathrm{m}^{-2}\mathrm{s}^{-1}$ when considering the MSW effect. This corresponds to a signal rate of 6.8 TNU and 6.2 TNU respectively for Thorium. The total predicted signal rate is therefore (31.3 ± 1.8) TNU when ignoring any matter effects or (28.5 ± 7.8) TNU when considering the MSW effect.

For comparison the flux with no neutrino mixing is predicted to be $(5.11 \pm 0.62) \times 10^{10}\mathrm{m}^{-2}\mathrm{s}^{-1}$ due to Uranium and $(4.52 \pm 0.54) \times 10^{10}\mathrm{m}^{-2}\mathrm{s}^{-1}$ due to Thorium. This would correspond to a geo-neutrino signal of (57.2 ± 9.7) TNU. A map of the predicted geo-neutrino flux at all points on the Earth surface, due to Uranium only and when assuming no mixing, was produced with 2x2° resolution and is seen in figure 3. The exact flux as predicted for key locations including those where prior geo-neutrino studies have taken place are shown in table 3.

4. Discussion

We presented a prediction of the geo-neutrino flux, and corresponding signal that will be seen, once SNO+ begins taking results in the previous section. A first evaluation of the credibility of the results can be obtained by comparing those produced in this study to those listed in similar studies carried out previously. In an alternative study by Fogli *et al* [18] a signal rate of (47.86 ± 3.23) TNU is reported. However this value is predicted based on an antineutrino detection efficiency of 1. If this assumption is applied to the results obtained in this study, the total signal rate rises to (45.6 ± 2.7) TNU for the

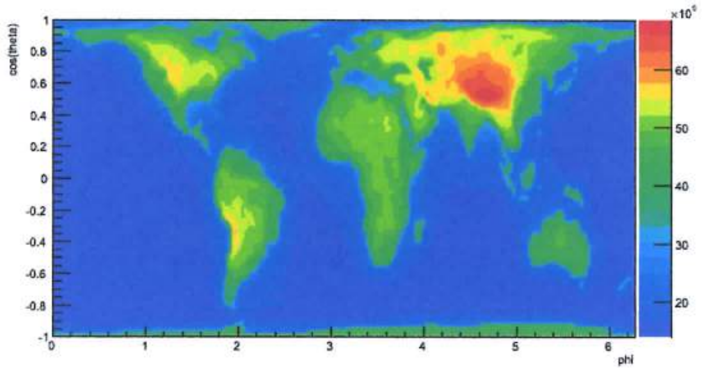

Figure 3: The predicted flux due to Uranium at locations across the Earth neglecting the effects of neutrino mixing. The colour scale is in units of $m^{-2}s^{-1}$.

Location	Flux ($10^{10}m^{-2}s^{-1}$)			
	Uranium		Thorium	
	Vacuum Mixing	MSW Mixing	Vacuum Mixing	MSW Mixing
Sudbury (46.5N,81.2W)	2.80 ± 0.12	2.55 ± 0.50	2.47 ± 0.10	2.25 ± 0.43
Gran Sasso (42N,14E)	1.89 ± 0.12	1.71 ± 0.50	1.63 ± 0.09	2.98 ± 0.51
Kamioka (36N,137E)	1.95 ± 0.10	1.77 ± 0.39	1.67 ± 0.08	1.51 ± 0.32
Central Australia (25S,133E)	2.63 ± 0.47	2.42 ± 0.48	2.30 ± 0.37	4.25 ± 0.48
Himalayas (33N,85E)	3.68 ± 0.53	5.09 ± 0.59	3.30 ± 0.45	3.03 ± 0.47
Hawaii (20N,156W)	0.79 ± 0.21	0.72 ± 0.21	0.59 ± 0.15	0.81 ± 0.19

Table 3: The geo-neutrino flux as predicted at key locations on the Earth surface

vacuum mixing case, which is in good agreement with the prediction made by Fogli *et al.* Similarly the signal predicted at Sudbury ignoring detection efficiency was given as (49.5 ± 7.4) TNU in [27]. This strongly suggests that the methods used within this study to predict the geo-neutrino signal are to the best of our knowledge reliable. The geo-neutrino signals at the three locations of the current neutrino observatories as predicted by this and previous studies are shown in table 4. While good agreement is observed between the predictions at both Sudbury and Kamioka, the signal obtained for Gran Sasso appears to be lower than those predicted elsewhere. One possibility is that this may be due to the use of different HPE abundance estimates.

The signals predicted for both Kamioaka and Gran Sasso can also be compared to the experimental results obtained by the KamLAND and Borexino experiments respectively. The results reported for KamLAND in [9] list a geo-neutrino signal rate of 51^{+39}_{-36} TNU. If assuming a detection sensitivity of 0.687, the results obtained in this study correspond to a signal rate of (21.7 ± 1.5) TNU. Therefore the results are in agreement, although the large relative uncertainty on the result reported by KamLAND diminishes the relevance somewhat. A recent, but as of the time of writing unpublished, report by Bellini *et al* of the Borexino collaboration proposes a detected geo-neutrino signal rate of (38.8 ± 12) TNU [28]. In this report, a detection efficiency of 0.84 ± 0.01 is claimed, and if this is applied to results of this study

Location	Geo-neutrino Signal (TNU) Mantovani *et al* [27]	Fogli *et al* [18]	This study
Sudbury	49.5 ± 7.4	47.86 ± 3.23	45.6 ± 2.7
Gran Sasso	40.4 ± 6.3	40.55 ± 2.86	30.6 ± 2.6
Kamioka	34.7 ± 5.7	31.60 ± 2.46	31.5 ± 2.2

Table 4: A comparison of the geo-neutrino signals predicted by this study and previous studies at the locations of neutrino observatories, ignoring detection efficiencies.

a geo-neutrino signal rate of 25.7 ± 2.2 is obtained. Once again our prediction is in agreement with the results obtained from experiment.

A further analysis of the results can be obtained from studying the angular variation in the geo-neutrino flux. The flux due to Uranium arriving at SNOLAB as a function of incidence angle is seen in figure 4. For small values of θ the flux is uniform and small, as expected, as this direction points outwards through a small amount of continental crust so there is little variation in the flux. The flux reaches a maximum at values near $\theta = \pi/2$ which also follows logically as this direction will point along the crust, which contains the highest abundance of HPEs. The flux arriving from larger values of θ is smaller due to the fact that this direction looks along the centre of the Earth where either the abundance will be lower, as with the inner layers of the Earth, or the inverse square dependence on distance will cause the geo-neutrino flux to be greatly reduced as from the crust on the far side of the Earth. Apart from small anisotropies the flux is roughly independent of ϕ, the reason being that this angle is the rotational angle around the detector and the inner layers of the Earth are assumed spherically symmetric so it is only the crust that will contribute to variations with respect to this coordinate.

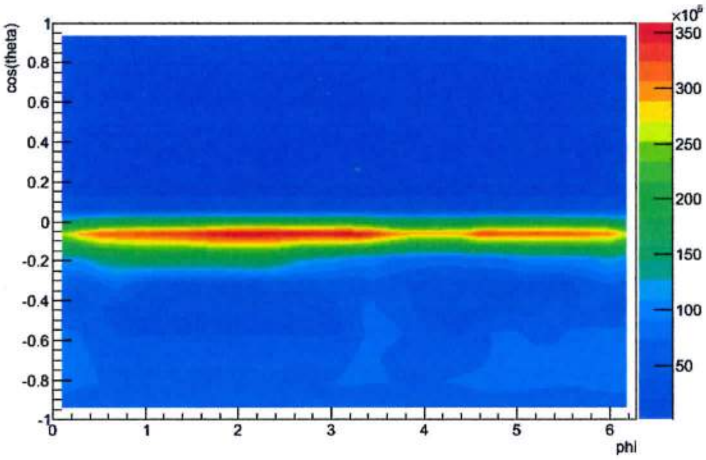

Figure 4: The predicted flux due to Uranium at SNOLAB as a function of incidence angle, neglecting the effects of neutrino mixing. The angle θ is defined such that it is the elevation angle from the axis which points directly to the surface of the Earth, while ϕ is the rotational angle measured from the axis pointing locally north. The colour scale is in units of $m^{-2}s^{-1}$.

The results show that the flux at SNOLAB will be much higher than that present at either the KamLAND or Borexino experiments. In theory a larger flux should be easier to detect and easier to separate from backgrounds, which would allow for a more accurate test of Earth models than previously available. However separating this signal from the backgrounds may not be simple. One possible source of fake signals could be due to solar antineutrinos. It is believed that if the neutrino is a Majorana particle, that is its particle and antiparticle are identical, and it possesses a magnetic moment there may be a process whereby a measurable solar antineutrino flux is produced. This flux is given as $\phi_{\bar{\nu}}^{Sol} < 3.8 \times 10^{-3}\phi(^{8}\mathrm{B})$ based on data from the KamLAND experiment [29] where the solar flux due to the ^{8}B decay is given in [30] as $\phi(^{8}\mathrm{B}) = 5.05 \times 10^{6}\mathrm{cm}^{-2}\mathrm{s}^{-1}$. Combining these results one obtains a solar antineutrino flux of $\phi_{\bar{\nu}}^{Sol} < 1.9 \times 10^{8}\mathrm{m}^{-2}\mathrm{s}^{-1}$, which is roughly 0.5% of the geo-neutrino flux predicted at SNOLAB so this effect should be small but is nonetheless worth considering.

As mentioned previously another significant source of fake events is those due to the decay of contaminants that have entered the detector. While the process of searching for the coincidence between two events for the detection of geo-neutrinos reduces the chance that scintillation caused by sources other than antineutrinos will result in fake signals, there are some interactions that can mimic this geo-neutrino signal. Neutrons with kinetic energy of a few MeV can ionize hydrogen atoms within the detector creating scintillation light, and will then later be captured by protons creating a second signal, similar to that observed for the inverse beta decay interaction of antineutrinos. In order for this effect to be a significant hindrance on the observation of geo-neutrinos, there needs be a suitably large source of these so called fast neutrons. One possible source was touched on previously, the (α, n) interactions whereby an alpha particle interacts with a low mass isotope within the detector emitting a free neutron. To cause a meaningful effect this in turn requires a large number of alpha producing radioisotopes within the detector. In a master's thesis it was noted that the most significant source of alpha particles in the detector at KamLAND with energy high enough to create neutrons was ^{210}Po which originated from the decay of ^{210}Pb [31]. The alpha particles from this decay have an energy of 5.3MeV which leaves just three isotopes, that will be contained within the liquid scintillator, with a threshold low enough to undergo this (α, n) interaction, ^{13}C, ^{17}O and ^{18}O. Based on their natural isotopic abundances, ^{13}C is by far the most common of the three isotopes so it is this that will cause the greatest number of fake events. Overall in the master's thesis it is proposed that the total signal rate due to the $^{13}\mathrm{C}(\alpha, n)^{16}\mathrm{O}$ interaction within the detector will be 106 TNU. This is a considerable effect when considering the predicted geo-neutrino signal and demonstrates the need for purification, it may however still be possible to detect the geo-neutrino signal on top of this background if it is well constrained. The last major form of backgrounds is that due to reactor antineutrinos. In [31] the reactor antineutrino signal rate at SNOLAB within the geo-neutrino energy range is predicted to be 44 TNU when using an average survival probability of 0.57.

While the results presented in this study are in general in good agreement with both previous predictions and experiments there are refinements that could be made in order to more accurately predict the geo-neutrino flux and signal. The most prominent area for improvement is in the Earth model, particularly for the inner layers. Due to both the age of the preliminary reference Earth model and its isotropic assumption one would initially assume a large amount of improvement could be gained via refinement. However when we considered only the crustal layers of the Earth the flux at SNOLAB was found to be roughly 78% of the total, suggesting that unless the inner layers nearest to Canada are considerably deviant from those predicted by the PREM, improvements to this area of the model is unlikely to yield much improvement. On the other hand corrections to the local area around the detector in both density and HPE abundance would almost certainly improve the results; in [31] it is noted that roughly 60% of the geo-neutrino flux at Sudbury originates within 500km of the detector. This area is described by just a few $2 \times 2°$ tiles, so by increasing the resolution within this area improvements in the result would follow. Additionally Canada is well known to have large deposits of Uranium, which are not described by our radial HPE abundance model, and would certainly impact the geo-neutrino flux arriving at the detector.

It is also worth discussing the result that including the MSW effect had on the geo-neutrino flux. For the majority of locations the flux predicted using the MSW effect was reduced by around 9% when compared to vacuum mixing, as seen in table 3. However due to the large amount of time it took to run the MSW simulation, we were unable to reduce the uncertainty arising from the variation in the result of the numerical integration. Therefore the results obtained for the majority of locations are inconclusive; while they suggest a noticeable reduction in the geo-neutrino flux as caused by the MSW effect, it is one of questionable accuracy. Some of the locations seem to show a large increase in the geo-neutrino flux when considering the MSW effect. However these results do not appear to be consistent with one another, for example disagreement between the effect for Thorium and Uranium at a given location. This implies that it was caused by a lack of computation time resulting in poor numerical integration accuracy.

SNO+ is not the only experiment currently planned that will attempt to measure the geo-neutrino flux. Hanohano is a planned neutrino observatory to be located in Hawaii which will also be able to detect antineutrinos via the inverse beta decay [32]. While Hawaii is expected to receive a much smaller geo-neutrino flux, we predicted a flux of $(0.79 \pm 0.21) \times 10^{10}\text{m}^{-2}\text{s}^{-1}$, it does have certain benefits. The absence of nuclear reactors significantly reduces the background, and the relatively small effect that continental crust has on the geo-neutrino signal reduces the effect that it's uncertainty has on the expected signal rate. Another detector being planned is the Low Energy Neutrino Astronomy (LENA) detector [33]. Although the exact location has yet to be decided it will likely be located in either Finland or France, with the aim to find a location that will reduce the backgrounds from reactors and cosmic rays to as great an extent as possible. This detector will be the largest neutrino observatory yet containing 50kton of liquid scintillator which should vastly increase the detection sensitivity.

5. Conclusion

The geo-neutrino flux is of fundamental importance in geophysics as it allows us to probe the Earth at a much deeper level than is available through direct measurement. Furthermore it makes possible one of the few available methods of quantifying the source of the Earth's internal heat. The source of the Earth's heat is of great value as it will enable a more detailed image of the history of the Earth and indeed information as to it's future. Additionally as geo-neutrinos originate from HPEs it remains to be seen whether, with the advance in neutrino detectors, positional dependant fluxes become available and as such help to yield the location of deposits of HPEs within the crust. Finally it may also be possible to detect geo-neutrinos originating from the decay of Potassium in the future via alternative interactions such as electron scattering, this interaction would have the added benefit that the direction of the scattered electron would be parallel to that of the incident neutrino, allowing a direct measure of the directional geo-neutrino flux.

In this study we used a numerical integration routine to predict both the geo-neutrino flux and signal that will be observed once SNO+ begins taking measurements. We used a combination of the PREM and CRUST2.0 models in order to define the density throughout the Earth and conducted a thorough review to find the current best estimates for the abundances of HPEs. The results obtained demonstrated good agreement with both previous predictions and experiments at different locations. We predict a geo-neutrino signal rate of 45.6 ± 2.7 TNU at SNO+; this is larger than the predicted signal rate at either KamLAND or Borexino and as such reinforces the suggestion that SNO+ will be able to gain the most accurate measurement of the geo-neutrino flux to date. While the backgrounds due to nuclear reactors and α contamination may present a significant hindrance, it is believed that this effect should be smaller than that for the previous experiments. Therefore the results that SNO+ obtains with regards to geo-neutrinos will help immensely to further constrain the effect that HPEs have on the heating of the Earth.

We have also presented an implementation of the MSW effect for geo-neutrinos, assuming an average Earth density for each antineutrino, and found that there is likely a slight reduction in the expected flux due to the result it has on the antineutrino oscillations. However the implication of this effect is limited due to a lack of computation time and as such further work is needed to test whether this will be a significant and measurable effect in the detection of geo-neutrinos. This is an exciting time for geo-neutrino physics, as more experiments are conducted across the globe the variation in the geo-neutrino flux can be further constrained to achieve an increasingly accurate image of the distribution of HPEs within the Earth.

6. Acknowledgements

I would like to thank Dr Rose for his continual assistance and advice throughout this project. Additionally I am grateful to Matthew Briggs for his work in calculating the geo-neutrino energy spectrums.

7. References

[1] S. M. Bilenky, Neutrino, PHYSICS OF PARTICLES AND NUCLEI 44 (1) (2013) 1–46. doi:10.1134/S1063779613010024.

[2] H. Bethe, R. Peierls, The "neutrino", NATURE 133 (1934) 532. doi:10.1038/133532a0.

[3] C. Cowan, F. Reines, F. Harrison, *et al*, DETECTION OF THE FREE NEUTRINO - CONFIRMATION, SCIENCE 124 (3212) (1956) 103–104. doi:10.1126/science.124.3212.103.

[4] G. Eder, Terrestrial Neutrinos, Nuclear Physics 78 (3) (1966) 657–&. doi:10.1016/0029-5582(66)90903-5.

[5] H. N. Pollack, S. J. Hurter, J. R. JOHNSON, Heat flow from the Earth's interior: Analysis of the global data set., Reviews of Geophysics 31 (3) (1993) 267–280. doi:10.1029/93RG01249.

[6] W. F. McDonough, R. Arevalo, Jr., Uncertainties in the composition of Earth, its core and silicate sphere, in: Adams, J and Halzen, F and Parke, S (Ed.), XXIII CONFERENCE ON NEUTRINO PHYSICS AND ASTROPHYSICS, Vol. 136 of Journal of Physics Conference Series, IOP PUBLISHING LTD, DIRAC HOUSE, TEMPLE BACK, BRISTOL BS1 6BE, ENGLAND, 2008, 23rd International Conference on Neutrino Physics and Astrophysics, Christchurch, NEW ZEALAND, MAY 25-31, 2008. doi:10.1088/1742-6596/136/2/022006.

[7] G. Fiorentini, M. Lissia, F. Mantovani, Geo-neutrinos and earth's interior, PHYSICS REPORTS-REVIEW SECTION OF PHYSICS LETTERS 453 (5-6) (2007) 117–172. doi:10.1016/j.physrep.2007.09.001.

[8] V. Lozza, S. Collaboration, Scintillator phase of the SNO plus experiment, in: Oberauer, L and Raffelt, G and Wagner, R (Ed.), 12TH INTERNATIONAL CONFERENCE ON TOPICS IN ASTROPARTICLE AND UNDERGROUND PHYSICS (TAUP 2011), PTS 1-6, Vol. 375 of Journal of Physics Conference Series, Max Planck Inst Phys (MPP); Tech Univ Munich (TUM); Origin & Struct Universe, IOP PUBLISHING LTD, DIRAC HOUSE, TEMPLE BACK, BRISTOL BS1 6BE, ENGLAND, 2012, 12th International Conference on Topics in Astroparticle and Underground Physics (TAUP), Munich, GERMANY, SEP 05-09, 2011. doi:10.1088/1742-6596/375/4/042050.

[9] T. Araki, S. Enomoto, K. Furuno, *et al*, Experimental investigation of geologically produced antineutrinos with KamLAND, NATURE 436 (7050) (2005) 499–503. doi:10.1038/nature03980.

[10] G. Bellini, J. Benziger, S. Bonetti, *et al*, Observation of geo-neutrinos, PHYSICS LETTERS B 687 (4-5) (2010) 299–304. doi:10.1016/j.physletb.2010.03.051.

[11] Online, Japanese evaluated nuclear data library (nov 2012).
URL `http://wwwndc.jaea.go.jp/jendl/jendl.html`

[12] S. Harissopulos, H. Becker, J. Hammer, *et al*, Cross section of the C-13(alpha,n)O-16 reaction: A background for the measurement of geo-neutrinos, PHYSICAL REVIEW C 72 (6). doi:10.1103/PhysRevC.72.062801.

[13] A. Dziewonski, D. Anderson, PRELIMINARY REFERENCE EARTH MODEL, PHYSICS OF THE EARTH AND PLANETARY INTERIORS 25 (4) (1981) 297–356. doi:10.1016/0031-9201(81)90046-7.

[14] G. Laske, G. Masters, C. Reif, A new global crustal model at 2x2 degrees (nov 2012).
URL `http://igppweb.ucsd.edu/ gabi/crust2.html`

[15] T. Plank, C. Langmuir, The chemical composition of subducting sediment and its consequences for the crust and mantle, CHEMICAL GEOLOGY 145 (3-4) (1998) 325–394, Workshop on Geochemical Earth Reference Model, LYON, FRANCE, MAR, 1996. doi:10.1016/S0009-2541(97)00150-2.

[16] R. L. Rudnick, S. Gao, The Crust, Elsevier, 2003, Ch. Composition of the Continental Crust.

[17] R. Rudnick, D. Fountain, NATURE AND COMPOSITION OF THE CONTINENTAL-CRUST - A LOWER CRUSTAL PERSPECTIVE, REVIEWS OF GEOPHYSICS 33 (3) (1995) 267–309. doi:10.1029/95RG01302.

[18] G. L. Fogli, E. Lisi, A. Palazzo, *et al*, Geo-neutrinos: A systematic approach to uncertainties and correlations, EARTH MOON AND PLANETS 99 (1-4) (2006) 111–130, Conference on Neutrino Geophysics, Univ Hawaii Manoa, Honolulu, HI, DEC 14-16, 2005. doi:10.1007/s11038-006-9107-5.

[19] Z. Maki, M. Nakagawa, S. Sakata, REMARKS ON THE UNIFIED MODEL OF ELEMENTARY PARTICLES, PROGRESS OF THEORETICAL PHYSICS 28 (5) (1962) 870–880. doi:10.1143/PTP.28.870.

[20] K. Zuber, Neutrino Physics Second Edition, CRC Press, 2011, p. 199.

[21] J. Beringer, J. F. Arguin, R. M. Barnett, *et al*, REVIEW OF PARTICLE PHYSICS Particle Data Group, PHYSICAL REVIEW D 86 (1). doi:10.1103/PhysRevD.86.010001.

[22] L. Wolfenstein, NEUTRINO OSCILLATIONS IN MATTER, PHYSICAL REVIEW D 17 (9) (1978) 2369–2374. doi:10.1103/PhysRevD.17.2369.

[23] G. Fogli, E. Lisi, Evidence for the MSW effect, NEW JOURNAL OF PHYSICS 6. doi:10.1088/1367-2630/6/1/139.

[24] K. Hagiwara, N. Okamura, K.-i. Senda, The earth matter effects in neutrino oscillation experiments from Tokai to Kamioka and Korea, JOURNAL OF HIGH ENERGY PHYSICS (9). doi:10.1007/JHEP09(2011)082.

[25] C. Rothschild, M. Chen, F. Calaprice, Antineutrino geophysics with liquid scintillator detectors, GEOPHYSICAL RESEARCH LETTERS 25 (7) (1998) 1083–1086. doi:10.1029/98GL50667.

[26] D. Wilkinson, ANALYSIS OF NEUTRON BETA-DECAY, NUCLEAR PHYSICS A 377 (2-3) (1982) 474–504. doi:10.1016/0375-9474(82)90051-3.

[27] F. Mantovani, L. Carmignani, G. Fiorentini, M. Lissia, Antineutrinos from Earth: A reference model and its uncertainties, PHYSICAL REVIEW D 69 (1). doi:10.1103/PhysRevD.69.013001.

[28] G. Bellini, J. Benzinger, D. Bick, *et al*, Measurement of geo-neutrinos from 1353 days of borexino.

[29] B. Chauhan, J. Pulido, E. Torrente-Lujan, KamLAND, solar antineutrinos, and the solar magnetic field, PHYSICAL REVIEW D 68 (3). doi:10.1103/PhysRevD.68.033015.

[30] A. Bellerive, Review of solar neutrino experiments, INTERNATIONAL JOURNAL OF MODERN PHYSICS A 19 (8) (2004) 1167–1179, 21st International Symposium on Lepton and Photon Interactions at High Energies, Batavia, IL, AUG 11-16, 2003. doi:10.1142/S0217751X04019093.

[31] L. Chunlin, Sno+ and geoneutrino physics, Master's thesis, Queen's University (2007).

[32] M. Batygov, S. T. Dye, J. G. Learned, *et al*, Hanohano- Deep Ocean Observatory for Particle Physics and Geological Studies, in: Adams, J and Halzen, F and Parke, S (Ed.), XXIII CONFERENCE ON NEUTRINO PHYSICS AND ASTROPHYSICS, Vol. 136 of Journal of Physics Conference Series, IOP PUBLISHING LTD, DIRAC HOUSE, TEMPLE BACK, BRISTOL BS1 6BE, ENGLAND, 2008, 23rd International Conference on Neutrino Physics and Astrophysics, Christchurch, NEW ZEALAND, MAY 25-31, 2008. doi:10.1088/1742-6596/136/4/042002.

[33] M. Wurm, F. von Feilitzsch, M. Goeger-Neff, *et al*, THE PHYSICS POTENTIAL OF THE LENA DETECTOR, ACTA PHYSICA POLONICA B 41 (7) (2010) 1749–1764, Cracow Epiphany Conference on Physics in Underground Laboratories and Its Connection with LHC, Cracow, POLAND, JAN 05-08, 2010.